JOURNAL OF OPTOELECTRONICS AND ADVANCED MATERIALS Vol. 10, No. 5, May 2008, p. 1032 - 1037

Magneto-transport study on Quasi 1-D magnet of $Ca_3(Co_{1-x}M_x)_2O_6$ (M: Ni, Fe, V, Ti ; $x \leq 0.1$)

JIAOLIAN LUO[a, +], MAKOTO AIDA[+], KOJI YAMADA[+], ZENTAROU HONDA[+], TOSHIROU SAKAKIBARA*, TAKASHI TAYAMA*, ISAO J. OHSUGI**
[A, +]*Dept. Material Science, Grad School of Saitama University, Sakura-ku, 338-8570 Saitama, Japan*
**Inst. for Solid State Physics, University of Tokyo, 5-1-5 Kashiwanoha, Kashiwa, 277-8581 Chiba, Japan*
***Dept. Electronics, Salesian Politechnic, 4-6-8 Koyamagaoka, Machida, 194-0215 Tokyo, japan*
[A] on leave from Guizhou University, Guiyang, Guizhou 550025, P. R. China
Correspondence to Prof. Koji. Yamada
[+]Collaboration Center, Saitama University, 255 Shimo-ohkubo, Sakura-ku, 338-8570 Saitama, Japan:

Magneto-transport phenomena in $Ca_3(Co_{1-x}M_x)_2O_6$ (M: Ni, Fe, V, Ti, $x \leq 0.1$) were investigated in a temperature range 12K-RT in dc fields up to 6T and pulsed magnetic fields up to 20T, respectively. The substitutions of Co with several metal M's were discussed by measuring magnetic susceptibilities and resistivities in the paramagnetic temperature range between of 77K-RT, to understand and apply the 3D physical natures. Future device of magnetic flip-flop is proposed by using the magnetic coupling formations of trigonal prisms.

(Received March 13, 2008; accepted May 5, 2008)

Keywords: Magneto-transport, magnetic susceptibility, Magnetic flip-flop

1. Introduction

A quasi one dimensional (q-1D) magnet of $Ca_3Co_2O_6$ was recently found by H. Fjelvag et.al.in 1996 and 1997 [1,2], which was attractive for material scientists. This is due to the following facts that the single crystal is acicular shaped, that the material exhibited spin glass behaviour in a cryogenic temperature range lower than 12K and that the electronic transport mechanism is proposed as 1D in addition to that of magnetism [3,4,5]. Characteristic magnetization plateau at 1/3 and 3/3Ms and not at 2/3Ms were found for the saturation magnetization Ms [4]. Attractive feature of this material was given rise by another stoichiometric crystal of $Ca_3Co_4O_6$ with a large conductivity and the large Seebeck coefficient in $Ca_3Co_4O_9$ with large and well 2D shaped crystals [6,7]. In this study, we observed magnetization and magneto-transport phenomena for samples of acicular crystals of $Ca_3(Co_{1-x}Mi_x)_2O_6$ (M: Ta, Fe, Ni, V metallic atoms, respectively), in long pulsed fields up to 20T and in a wide temperature range between 10 K-285 K [8]. We aimed at the future application of the characteristic behaviours of the magnetization and the electronic transport properties as nano-scaled electronic devices. For these purposes, we performed crystal growths of many samples with different metals M and composition $x \leq 0.1$. Further, the specific experimental apparatus of the pulsed high field magnet was set-up with a long half-width pulsed field of 30ms to avoid magnetization delay and also to prevent the crash of the sample mount made of Cu-pipe, caused by large Eddy current. The photographs of the samples are demonstrated for the real information of the sample growth by flash method. The study of the magnetic properties of one dimensional magnet has been a physical subject for a long time, particularly that exhibiting a magnetic phase transition from quasi 1-D ferromagnetism with intra-chain ferromagnetic coupling, to 3-D paramagnetism at higher temperature range around at 24 K. $Ca_3Co_2O_6$ crystallizes in hexagonal lattice with space group *R-3c* and lattice parameters *a*=0.907.3 nm and *c*=1.038.1nm at 298 K. The crystal structure of $Ca_3Co_2O_6$ is precisely explained in the researchers [1,2]. $Ca_3Co_2O_6$ consists of infinite chains of alternating face sharing CoO_6 trigonal prisms with high spin of 3 μ_B and CoO_6 octahedra with low spin of 0.08 μ_B along the hexagonal *c*-axis. The inter-chain distance is 0.5240nm, which is about twice as large as the intra-chain Co distance of 0.259 nm. Each CoO_6 chains formed a triangular network perpendicular to the *c* axis which shows very characteristic magnetization curve of 1/3Ms plateau for the saturation magnetization of Ms where the triple-fold degenerated spin states exhibits the possible state of M=0 at B=0, 1/3Ms, Ms without 2/3Ms in a specific temperature range between 12 K-24 K [9,10,11], and in a magnetic field range smaller than about 6T Further, the electronic conduction shows 1-D nature in a temperature range between 12 K and 50 K [5] and above in this temperature range, it shows conventional 3D nature.

2. Experimental procedures

2.1 Sample preparations

We grew many kinds of single crystals of $Ca_3Co_2O_6$ and $Ca_3(Co_{1-x}M_x)_2O_6$ (M: mostly metal or general atoms) were synthesized as follows. Mixtures of $CaCO_3$, MCO_3 and CoO with the ratio $(Ca_{1-x}M_x)$:Co =3 : 2 were heated at 1000K for 48h in air. Single Crystals of $Ca_3Co_2O_6$ and $Ca_3(Co_{1-x}M_x)_2O_6$ were grown by usual flux method

using flux of KCO_3 reported in Ref.[7]. Acicular crystals of 10 mm length or longer were obtained by the following method. First, the intermediate product of powder, $Ca_3(Co_{1-x}M_x)_2O_6$ was twice obtained by baking the mixture of $CaCO_3$ and CoO with the ration of Ca:Co=3:4 or arbitrary oxide M as $Co_{1-x}M_x$, (e.g. in case of M=Ni, x=0.1; $CaCo_3$: NiO=15:18.2) in the air for 24 hrs at 900 °C as shown in the heating program is shown in Fig. 1(a), upper figure. After baking, the intermediate materials was once grained into powder in a bowl for 1 hours. The final acicular crystals were grown by the flux method using the intermedaite material of $Ca_3Co_4O_9$ with K_2CO_3 in the ratio of 1:7 in the same electric furnace for 48 hours with the time sequence program as shown in Fig. 1(a), lower figure. The plate shaped crystals, composed of $Ca_3(Co_{1-x}M_x)_4O_9$, in the same crucible was sometime obtained as a bi-product. The plate-shaped crystal (2-D) includes some miss-fit atomic layers, which show large Seebek coefficients [12]. Fig. 1(b) shows the typical sample shapes of the as-grown single crystals. Both S-1 and S-2 show glittering surface and the ratio of the length (l) and diameter (d) :l/d are at least 100 or more. We compared the X-ray diffractions in powder of the single crystals with simulations (RIETAN-2000) where major peeks are shown in Fig. 3. It is apparent that the prepared samples with different M (V, Ti, Fe, Ni) and x within 0.1 are almost the same together with that of pure single crystal and that of the simulation in a good coincidence. In the later section, we show the results of magnetizations in connection with the resistivities of the samples with different M.

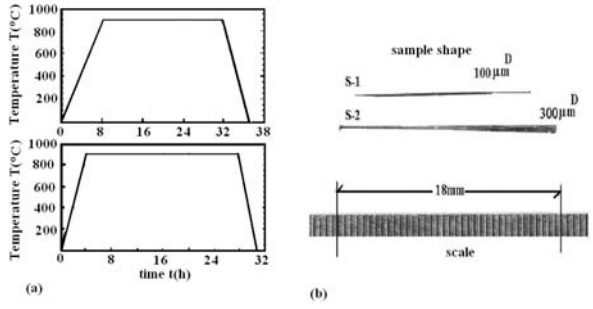

Fig. 1. Heating program of the sample preparations (a) and the sample shape (b).

2.2 Measurements of resistivity and magneto-resistance

We performed the measurements of sample resistance under the zero magnetic field in a temperature range between 77 K and RT to avoid 1-D nature as explained in the introduction, and magneto-resistance in pulsed high fields up to 20T in a temperature range between 10 K and RT for stoichiometric and non-stoichiometric samples. Fig. 3(a) shows the experimental results of the sample resistivities with different M as a function of temperatures between 100 K and RT. Fig. 3(b) shows the same resistances for the samples in Fig. 3(a) as a function of $(T)^{-1/4}$ in comparison with the resistances for samples of $Ca_{3-x}Y_xCo2O6$ in Fig. 3(c) to compare the slope of the other type of substitutions [12]. The stoichiometric sample (pure sample) showed lower resistivity than that of M=Fe and showed larger resistivities than those substituted samples by Ni, V, Ti in this order [13]. All these resistivities increased with decreasing temperature in the same manner as that in semiconductors. Here, for a sample with M=Ni, the resistivity decreased with increasing x up to 10% in this experimental extent, whereas the resistivity already become unchanged for a sample with M=Ti up to x=10%. We performed the measurements of magneto-resistance for a sample with M=Ni, x=0.1 in a wide temperature range between 10K and RT in pulsed high magnetic fields up to 20T with a long half-width of 30ms[11]. In this experiment, we used analogue to digital converter (ADC) with 4 μs/Word, 32 kW up to 120 ms. For examples, we show the results in Fig. 4 where a small negative magneto-resistance of 0.2% was observed in a paramagnetic temperature T=88 K, B=20T, and also observed more than 10% at T=14 K, B=20T in B//C//I configuration, respectively. It is worth whole to note that between 10 K-24 K, the magneto-resistance shows very peculiar characteristic as shown in Fig. 4(r.h.s). It must be noted here again that at T=88K, the electronic transport phenomenon shows 3-D nature, and magnetic property, at 14 K shows 1-D nature [5].

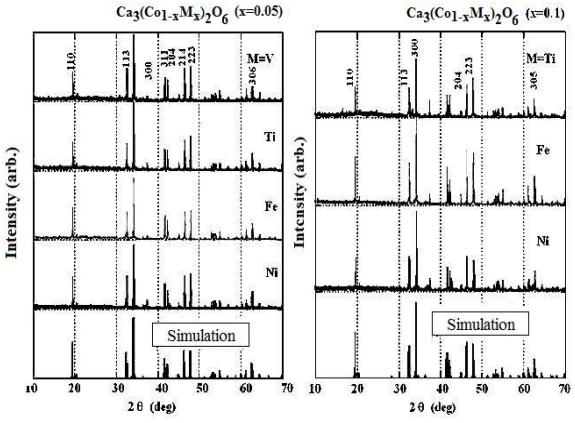

Fig. 2. Experimental X-ray diffraction intensities of powder crystals with different M and x=0.05, x=0.1, and of simulation at the bottom figures.

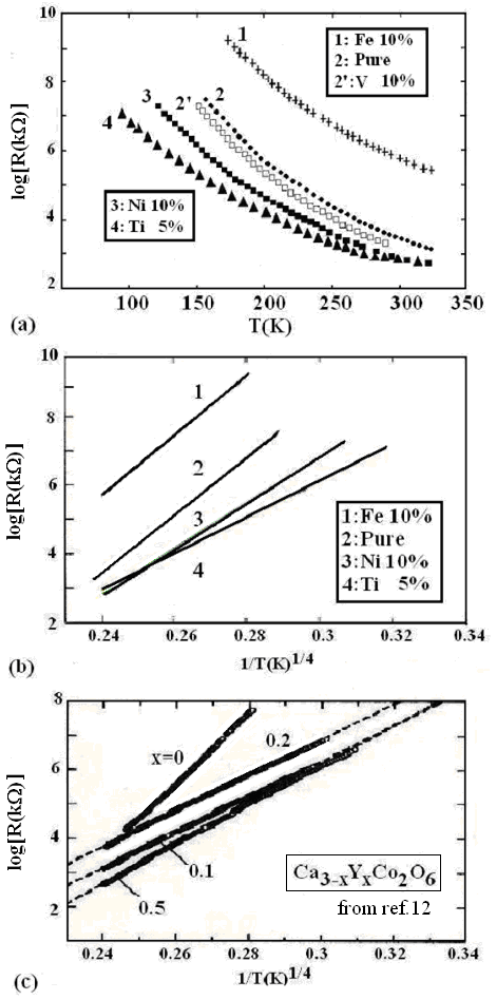

Fig. 3. Specific resistivities of samples with variously substituted samples (a) as a function of T, (b) as a function of $T^{-1/4}$ and (c) the resistivities of the samples: $Ca_{3-x}Y_xCo_2O6$ as a function of $T^{-1/4}$ (T. Sekimoto et.al. [12]).

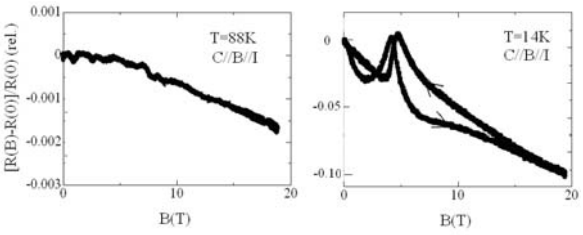

Fig. 4. The typical behaviors of magneto-resistance of a sample with M=Ni, x=0.1 at T=88K and that at T=14K in pulsed fields up to 20 T with a long half-width of 30 ms.

2.3 Measurement of magnetizations in dc fields

Because the magnetization of this material in pulsed fields showed large time delay inevitably [8], we performed magnetization measurements in d.c. fields up to 6 T as shown in Fig. 5 together with the schematic figure of magneto-resistance in dc fields and in pulsed fields obtained from that in Fig. 4. The pure sample showed the saturation magnetization of 75 emu/g (Ms) and many kinks in the magnetization curve as a function of dc fields at 4K, caused by spin column formations more than three with ferromagnetic intra-chain and anti-ferromagnetic inter-chain interactions. Here, the spin columns are arbitrarily interact and connected with the nearest columns and re-form the new column network in each magnetization due to small perturbations by lattice vibrations. In between 10 K-25 K, the spin chain interactions are limited within a triangle-formed interactions among ferromagnetic intra-chains and anti-ferromagnetic inter-chains. Here, the spin columns are disconnected except the nearest triangle spin formation. It is noted here that at these temperatures, there is no stable magnetization at 2/3Ms as is apparently shown at T=15 K. In the bottom of this figure, MR at T=15 K in pulsed fields, MR is schematically shown in comparison with the magnetization measurements and also MR in d.c. fields. It must be noted here that MR sharp maximum was observed in B=3.6 T at T=15 K, which corresponds to 2/3Ms.

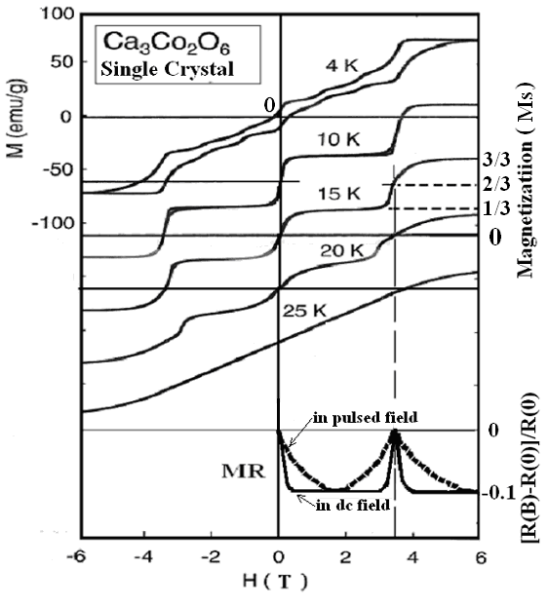

Fig. 5. Magnetization as a function of dc fields at different temperatures and MR at T=15K in dc fields and pulsed fields under 15 K at the bottom.

2.4 The paramagnetic susceptibility

To know the atomic positions of the substituted material M, we performed the measurements of the paramagnetic susceptibility of samples with Ni, x=0.1 in comparison with that for a pure sample, in the temperature range between 100 K and 300 K as shown in Fig. 6. Here experimental values are shown by open triangles and squares for the samples with (x=0) and with M=Ni, x=0.1, respectively. The solid curves shows the Curie-Weiss

equation for each sample as a function of temperature T as

$$\chi = \frac{C}{T - \Theta} \quad , \tag{1}$$

with the best fitting values of C=3.16,Θ =18.8 for the pure sample, C=2.48, Θ =18.7 for a sample with M=Ni, x=0.1, respectively [13]. Here, we adopted the theoretical paramagnetic magnetization given by Brillouin function B_S as

$$\chi = \frac{Ng_J\mu_B S}{H} B_S\left(\frac{g_J\mu_B SH}{k_B T}\right), \tag{2}$$

$$B_S(x) = \frac{2S+1}{2S}\coth\left(\frac{2S+1}{2S}x\right) - \frac{1}{2S}\coth\left(\frac{x}{2S}\right). \tag{3}$$

Here, N stands for mole number, S, the effective spin number, H, the magnetic field, etc. We discuss on the adopted values of these quantities in the next sections.

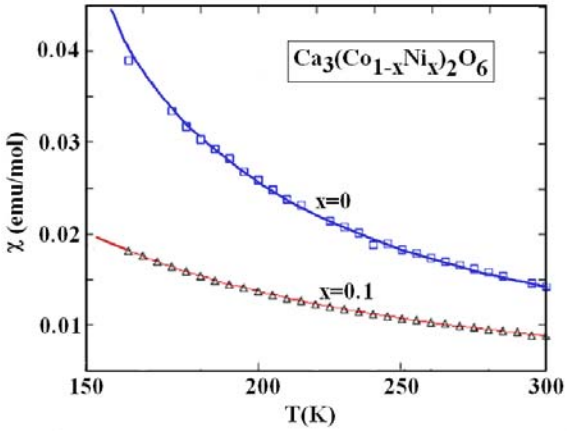

Fig. 6. Experimentally obtained magnetic susceptibilities as a function of temperatures for the two samples of a pure and a doped ample with (M=Ni, x=0.1), respectively in comparison with the theoretical functions (solid lines).

3. Discussion

We showed experimentally obtained resistivities of samples with different M (V, Fe, Ni. Ti) and x(0<0.1) in a paramagnetic temperature range above 77 K or in the resistivity range smaller than 10^8 Ohm·cm, limited by the technical problem for measurements. In these limited conditions, we avoided the complex physical interpretations of low dimensional conduction mechanism in the cryogenic temperature range lower than 50 K where 3-D to 1-D occurs.

It is apparent that the substitution of Ni with Co showed the smaller resistivity and smaller magnetization as shown in Fig. 3(a) and Fig. 6. The sample resistivities with M=Ti^{4+}($3p^6$, r=0.46nm, x=0.05 and 0,1) in Fig. 3(a) showed rather complex dependence on x. In this case, the resistivities dropped remarkably for the sample with x=0.05 and stopped decrease or saturate in the sample with x=0.1.The ion radius of Ti is small enough to substitute Co^{3+} both in prism and/or octahedron. This might cause the large electronic vacancies for hopping conduction with the lower activation energy (E_A) of 0.154 eV (1790 K) than that of the pure sample, 0.287 eV (3340K) by adopting an assumption that the resistivity $R \approx exp(-E_A/k_BT)$. This anomalous resistivity change also observed in $Ca_{3-x}Y_xCo_2O_6$, where the Y substituted both with low spin Co sites (prism) and high spin Co site (octahedron). In both cases, the activation energies become smaller due tot the wider hopping sites than those in 3D via from Co^{2+}(e_g orbit) to O^{2-}(2p orbit) vice versa. In any case we found lower resistivities than that for the pure sample or stoichiometric state without lattice voids (see Table 1). The sample with M=Fe^{3+} shows the larger resistivity with the lower activation energy might be plausible due to the filling of the electronic vacancies by the extra electron from Fe^{3+}.

Table 1.

$Ca_3(Co_{1-x}M_x)_2O_6$

M: x	0	Fe: x=0.1	Ni: x=0.1	Ti:x=0.05
Δ / K	3095	3046	1994	1790
Θ	18.8		18.7	

$Ca_{3-x}Y_xCo_2O_6$

Y: x	0	0.1	0.2	0.5
Δ / K	3340	1586	1709	1871
Θ	20.46	19.81	13.71	1.79

(from ref,12)

Now, we discuss the possibility of the substituted positions of Ni in a small x range less than 0.1. The high spin state of Co^{3+}($3d^6$), S=2 could be partially replaced with Ni^{2+}($3d^8$), S=1, due to the closer ion radii (r) with that of Ni^{2+}(r=0.83 nm) in comparison with that of Co^{3+}(0.75 nm), high spin state in the trigonal prism (CoO_6), than the low spin Co^{3+} (r=0.69 nm) in octahedron of CoO_6. The experimentally obtained $\langle S\rangle_{exp}$ in Eq.2 and Eq.3 for the sample with M=Ni,=0.1 was determined at 1.78 in good accordance with the theoretical value $\langle S\rangle_{theor.}$=1.8, obtained by the given occupancies of the high and low spin Co^{3+} sites as n_{HCo}=0.4, n_{LCo}=0.5, respectively. On the other hands, the larger conductivity of the sample with M=Ni. x=0.1 than that of the pure sample, was explained by the vacancies of electrons caused by the smaller valence of Ni^{2+}. Further, the larger resistivity and the larger magnetization of the sample with M=Fe, x=0.1 than that of the pure sample, reflects the smaller mobile electrons by the larger valence of Fe^{3+}[6], and reflects the larger magnetization by the larger spin S=5/2 (Fe^{3+}, $3d^5$, r=0.79). Apparently, in this case, Fe^{3+} ions substitute the high spin Co site with the extra electron number larger magnetization and V^{5+} (r=0.68nm) substitutes Octahedron

site of Co^{3+} with the lower spin state. In this case, magnetization changed a little with those of a pure sample.

The MR observed for a sample with M=Ni,x=0.1 in pulsed fields and that in dc fields exhibited a big difference as shown in Fig. 4 and Fig. 5 at the bottom. The main reason might be caused by the frequency dispersion of the magnetizations. Namely, the quasi-1D magnetization propagates along the long linear chain of magnetic domains which are pinned by some defects at the center in Fig. 7(a). Namely, the propagation of magnetic linear domain need much longer time than that in 3D case. As depicted in Fig. 5, MR in dc fields shows a sharp maximal peak observed at the 2/3Ms. Even in dc field, the broadness of MR maximal peak is determined by the magnetization rise from 1/3Ms to 3/3Ms. This corresponds to the intensities of spin fluctuation at T=15 K in Fig. 5. Therefore, the magnetic domain could spatially confine within the length of spin voids. In the other words, for a sample with M=Ni, the domain size is controllable by x.

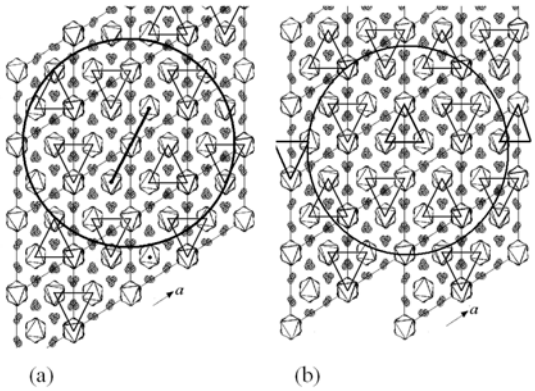

Fig. 7. The triangle spin array formations in (a x b)-plane (a) with line miss-fitting (b) without miss-fitting.

As is little mentioned, the triangle spin formation as shown in Fig. 7(b) is most plausible physical model in a temperature range between 12 K-24 K, where lattice disturbance of spin system determines the extent of the ferromagnetic interactions between chains. The magnetic susceptibility in dc field is largely dependent on the lattice defects or spin voids. In case of the perfect crystal, dc susceptibility might be large enough to cause the sharp maximum. In case of the pulsed fields with lattice imperfections, the M-H curve become slow rise due to the pinning of domain movements along c-axis.

In the end of this paper, we explain the spin states of the triple-fold degeneracy e.g. as $\Phi(\uparrow,\uparrow,\downarrow),\Phi(\uparrow,\downarrow,\uparrow),\Phi(\downarrow,\uparrow,\uparrow)$ along the positions α, β, γ, as shown in Fig. 8(a), where the spin clusters in c-axis are illustrated. These three states are degenerated by rotation symmetry of R_{3C}. Therefore, the spin state can flip from $\Phi(\uparrow,\uparrow,\downarrow)$ to $\Phi(\uparrow,\downarrow,\uparrow)$ by tunneling and realize the spin eigen-state of $\Phi(\uparrow,\uparrow,\downarrow)$ by pulling-up the spin at r=α and β with the final spin state "$(\downarrow)$" at r=γ as shown in Fig. 8(a). In this stage of our investigation, the pulling-up of specific spin could not be performed artificially in this material as it is. In the future study, using some foreign atom on Co^{3+} high spin site via super exchange interaction or direct ferromagnetic interaction, this kind of manipulation will be possible as in Fig. 8(b-1), (b-2) and (b-3).Here, the condition of pulling-up of electrons corresponds to the control of the logic by tunneling in a fast propagation velocity [14,15].

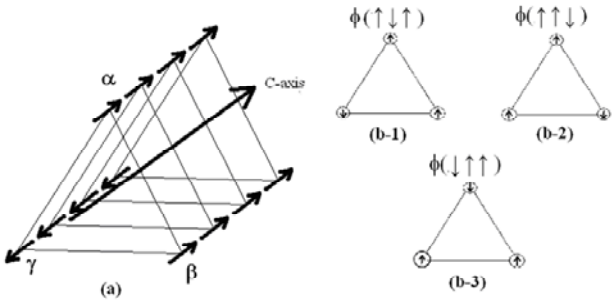

Fig. 8. The triangle spin array configuration in 1-D column (a) Schematic spin block along c-axis, (b) The triple-fold degeneracy of spin configurations with the same eigen energy.

The spin cluster size of the magnetic domain could be controlled by choosing M and x. As we already discussed, a sample with M=Ni^{2+} exhibited smaller hysteric behaviors than the research work by Raquet et.al. due to the smaller spin clusters in this study than that in pure sample with the longer intra-chain magnetic interactions. These hysteric behaviors could be understood in comparison with the MR behaviors in [5], where a large temporal delay of MR was found during the magnetic field sweep.

As discussed just above, the spin degeneracy denoted by R_{3c} could be resolved by using a small perturbation of any kinds of forces, in which each wavefunction could be discriminated by positions.

4. Conclusions

Magneto-transport study on $Ca_3(Co_{1-x}M_x)_2O_6$ were performed by choosing M and x. Here, the substitutions of high spin state $Co^{3+}(3d^6,S=2)$, is clarified by $Ni^{2+}(3d^8,S=1)$ with the smaller magnetization and the lower resistivity, and is by $F^{3+}(3d^5,S=5/2$ by the larger magnetization and the larger resistivity in proportional with $x \leq 0.1$. In case of Ti, ionic radii is too small that the interstitial or substitutional positions could be clarified, or both are possible. However, this sample showed the smaller resistivity than that for a pure sample and the lower activation energy in comparison with the other M.

An application in the future is proposed by using some degenerated wavefunction with spin part in this material. The physical tool to discrimination is open for discussion.

References

[1] H. Fjellvag, E. Gulbrandsen, S. Aasland, A. Olsen, B. C. Haubaek, J. Solid State Chem. **124**, 190-194 (1996).

[2] S. Aasland, H. Fjellvåg, B. Hauback**,** Sol. State Commn. **101**(3), 187-192 (1997).

[3] H. Kageyama, S. Kawasaki, K. Mibu, M. Takano, K. Yoshimura, K. Kosuge, Phys. Rev. Lett. **79**, 3258 - 3261 (1997).

[4] H. Kageyama, K. Yoshimura, K. Kosuge, M. Azuma, M. Takano, H. Mitamura, T. Goto, J. Phys. Soc. Jpn. **66**(12), 3996-4000 (1997).

[5] B. Raquet, M. N. Baibich, J. M. Broto, H. Rakoto, S. Lambert, A. Maignan, Phys. Rev. B **65**, 1044421 – 1044425 (2002).

[6] S. Bhattacharya, D.K. Aswal, A. Singh, C. Thinaharan Nilesh Kulkarni, S. K. Gupta, J. V. Yakhmi, J. Crystal Growth **277**(1-4), 15, 246-251 (2005).

[7] J. Luo, Doctor Thesis, Saitama Univ., March (2007), Investigation on pure single crystals of $Ca_3(Co_{1-x}M_x)_2O_6$ and magneto-resistances in high pulsed magnetic fields. ,in Japanese.

[8] K. Yamada, Z. Honda, J. Luo, H. Katori, J. Alloys and Comp. **423**(1-2), 26, 188-190 (2006).

[9] V. Hardy, D. Flahaut, R. Fresard, A. Maignan, J. Phys. Cond. Matt..**19**(14), 14229-14237 (2007).

[10] J. Luo, K. Yamada et. al. J. Jpn. Soc. Appl. Eelectromagn. Mech. **15**(2), 156-161 (2007), in Japanese.

[11] H. Kageyama, K. Yoshimura, K. Kosuge, H. Nojiri, K. Owari, M. Motokawa, phys. Rev. B **58**, 11150-11152 (1998).

[12] T. Sekimoto, S. Noguchi, T. Ishida, J. Phys. Soc. Jpn. **73**(11), 3217-3218 (2004).

[13] M. Aida, Thesis for Bachelor, Investigations on properties of $Ca_3(Co_{1-x}M_x)_2O_6$ (M=Metal), Saitama University, March 2007, in Japanese

[14] A. Maignan, V. Hardy, S. Hebert, M. Drillon, M. R. Lees, O. Petrenko, D. Mc K. Paul, D. Khomskii, Quantum tunneling of the magnetization in the Ising compound $Ca_3Co_2O_6$, e-print (2004) 3695.

[15] C. H. kim, H. Kim, S. H. Park, J. Hyun Paik, J. H. Cho, B. G. Kim, Tuning of magnetic ordering by Y substitution in $Ca_3Co_2O_6$, J. Phys. Soc. Jpn, **74**(8), 2317-2322 (2005).

*Corresponding author: yamasan@fms.saitama-u.ac.jp